The Density Integration Approach to Populations. A Critical Comparison of Projection Populations to Populations Defined by the Theory of Atoms in Molecules

Rainer Glaser

Department of Chemistry, Yale University, New Haven, Connecticut 06511

Received 21 March, 1988; accepted 14 June, 1988

The theory of atoms in molecules defines an unambiguous partitioning of the three-dimensional electron density into atomic basins based on the zero-flux surfaces of the gradient of the electron density, $\nabla\rho(r)$. Integrations of the electron density within such basins yield integrated Bader populations (IBP) that have a rigorous foundation in quantum mechanics. In the density integration technique based on the two-dimensional electron density projection function, $P(x,z)$, integrated projection populations (IPP) are obtained by integration within regions demarked by steepest descent lines D_p of $P(x,z)$. These density integration techniques are compared by an analysis of the electron density of diatomic molecules that is based on the properties of the zero-flux surface that partitions the electron density between the atoms. The conventional method for the partitioning of regions of $P(x,z)$ approximates the virial partitioning. Differences between IPP and IBP can be quantitatively described by two terms. One term reflects the error intrinsic to projection populations as a result of the loss of all information about the electron distribution in the third dimension in the calculation of $P(x,z)$. The second term accounts for the effects of the displacement of the demarcation lines D_p toward the less polarizable atom compared with the cross-section of the density with the plane of projection, D_d. The analysis suggests the definition of a projection population IPP2 that is based on the cross-section D_d instead of the demarcation lines D_p. Relations between the populations IPP, IPP2, and IBP are derived for diatomic molecules and numerical results are presented for a series of diatomic molecules. Several polyatomic anions are also discussed. The values of IPP are found to be good approximations of IBP in highly polar diatomic molecules. In cases where the bonding involves comparatively little intramolecular charge transfer IPP2 is the better and equally satisfactory projection population. In the intermediate semipolar bonding situations projection populations provide qualitatively correct descriptions of the charge distributions but the numerical agreement with the IBP values is less satisfactory.

INTRODUCTION

The concept of *atomic charge* in molecules is one of the most useful tools for chemists to characterize the nature of bonding, to explain the reactivity of molecules, and to discuss reaction mechanisms. Yet, it has proved difficult to quantify the notion of *atomic charge* within the framework of quantum chemistry. The general problem of any population analysis consists in the partitioning of the electron density. Basis set partitioning and electron density integration techniques have emerged as the two fundamentally different approaches to determine populations.

Among the population analyses based on basis set partitioning are the Mulliken population (MP) analysis,[1] the SEN method (shared electron number),[2-4] and the natural population method[5] to name a few.[6] The Mulliken population analysis is the most usually applied method of this class and its capabilities and deficiencies are well known.[7-10] Density integration techniques differ from the basis set partitioning techniques fundamentally in that they consider only the electron density (as defined by the wave function). The electron density is experimentally observable and graphical representations can be studied to facilitate comparison, to reveal trends, and to express topological characteristics better than any print out. Problems arising in the basis set partitioning technqiues related to the assignment of density to the basis function centers do not occur. The problem of partitioning the electron density between the nu-

Journal of Computational Chemistry, Vol. 10, No. 1, 118–135 (1989)

CCC 0192-8651/89/010118-18$04.00

clei remains, and different methods have been proposed to resolve it. The partitioning of the electron density has been carried out with reference to the free atoms,[11-15] without reference to free atoms but to other assumptions,[16] and based exclusively on the topological features of the electron density. The latter approach has received its most rigorous and elegant treatment by Bader and co-workers.[17-32] The density integration technique developed by Streitwieser and coworkers is based on the topological features of electron density projection functions,[33-37] and has been applied routinely over the last decade to study a variety of theoretical organic problems.[33-39]

Here a comparison is presented between the density integration techniques of Bader and Streitwieser. The methods are briefly reviewed with emphasis on the partitioning schemes. Criteria are presented that allow for a qualitative description of the approximations intrinsic to the partitioning of projection functions compared with partitioning in three-dimensional space. In the main discussion of this article, relations between the integrated populations are derived for diatomic molecules based on the properties of the zero-flux surface of the gradient of the electron density $\nabla\rho(r)$. Integrated populations obtained with several partitioning methods are reported for a series of diatomic molecules to provide numerical evidence for and to test the conclusions of the analysis. Some polyatomic π-conjugated anions are also considered.

DENSITY INTEGRATION TECHNIQUES

The Bader Method

The studies of electron density distributions by Bader's group may be seen to proceed through three distinct stages. In the early articles[17] no attempt was made to partition the total electron density. The report by Bader, Beddall, and Cade[18] may be regarded as the beginning of the second phase.[18-22] A *natural partitioning* of the electron density was proposed[18] and defined by a plane perpendicular to the molecular axis and passing through the point at which the electron density reaches a minimum along the internuclear axis. The partitioning scheme was refined by Bader and Beddall,[19] and it was shown that it is possible to partition a molecule so that the virial relationship holds for the molecular fragments. This unambiguous spatial partitioning requires that the regions are connected by a surface $S(r)$ such that the flux of the gradient of the density, $\nabla\rho(r)$, normal to the surface be zero at every point on the surface. This partitioning method defines the atom in the molecule and provides the basis for the theory of atoms in molecules.[21,22]

The paper by Bader, Anderson, and Duke[23] on the quantum topology of the charge distribution may be regarded as the beginning of the third stage.[23-30] The basis for the topological characterization is given by the gradient vector field of the electron density, $\nabla\rho(r)$,[23-26] and by the Laplacian distribution of the density, $\nabla^2\rho(r)$.[27,28,40] The gradient vector field plays the central role in the partitioning of the density. *Critical points* in $\nabla\rho(r)$, points where $\nabla\rho(r) = 0$, define the principal characteristics of the electron distribution. These points are characterized by the non-zero eigenvalues λ_i of the Hessian matrix[23] of $\rho(r)$, that is, the principal curvatures of $\rho(r)$ at the critical point. The critical points are classified by the *rank*, denoting the number of non-zero eigenvalues λ_i and the *signature*, the number of excess positive over negative eigenvalues λ_i. Possible combinations of rank and signature are limited to the pairs (rank, signature): $(3,+3), (3,-3), (3,-1)$ and $(3,+1)$. Critical points $(3,+3)$ and $(3,-3)$ coincide with the interior of a cage and the position of the nuclei, respectively. Critical points $(3,+1)$ and $(3,-1)$ are saddle points and occur in the central position of a ring system or between bonded atoms, respectively. The unique trajectory traced out by $\nabla\rho(r)$, associated with the positive eigenvalue, and originating at the bond critical point in most cases[41] connects two bonded atoms and defines the *bond path*,[21,42] and the trajectories associated with the negative eigenvalues define the zero-flux surface that partitions the molecule into atomic fragments. In these terms, the set of surfaces generated by all $(3,-1)$ points partitions the space of a molecule into a collection of chemically identifiable atomlike regions, called *basins*. Numerical integration[25] of the electron density within the basins yields atomic populations. Aside from the definition of atomic popula-

tions based on quantum mechanics, the theory of atoms in molecules[29] has been applied to many other problems,[31,32,43–45] primarily by the groups of Bader, Wiberg, and Cremer.

Electron Density Projection Functions: The Streitwieser Method

Integrated projection populations (IPP)[46], are based on the electron density projection function $P(x,z)$,[34–36] that is defined by

$$P(x,z) = \int_{-\infty}^{+\infty} \rho(x,y,z)dy$$

For the discussion of the partitioning required to determine projection populations the following topological description of $P(x,z)$ is useful. Contour maps of $P(x,z)$ parallel density diagrams, and they may be described in a similar manner for planar molecule if the projection plane coincides with the molecular plane.[47] Using the gradient of the projection function, $\nabla P(x,z)$, and defining the *rank* and the *signature* in analogy to Bader et al.[23] the *projection critical points* $(2,-2)_p$, $(2,0)_p$ and $(2,+2)_p$ may be defined. Critical points $(2,-2)_p$ correspond to maxima of $P(x,z)$. The points $(2,0)_p$ correspond to saddle points of $P(x,z)$, and the points $(2,+2)_p$ occur in the centers of ring systems. As with the points $(3,-1)$ the critical points $(2,0)_p$ play a crucial role for the integration procedure.

Integration of the projection functions in regions around specified atoms leads to the IPP value.[37] The partitioning of $P(x,z)$ is done in an unambiguous manner; that is, a demarcation line is defined that originates at the critical point $(2,0)_p$ and follows the steepest descent path in both directions. The trajectory associated with the positive eigenvalue of $\nabla P(x,z)$ defines the *projected bond path* and the other trajectory defines the *demarcation line* D_p. For homonuclear diatomic molecules the critical points $(2,0)_p$ and $(3,-1)$ coincide, and the steepest descent path in two-dimensional space emulates a plane that is identical to the zero-flux surface of the gradient of the density. For all other cases this integration procedure gives values that are approximations to the integrated population of a *basin*.

RELATIONS BETWEEN INTEGRATED POPULATIONS

Criteria Describing the Approximations

Consider a diatomic molecule composed of atoms with a large electronegativity difference; LiCl is a good example. Given a wave function for this molecule[48] the $C_{\infty v}$ symmetric zero-flux surface, ZFS, can be determined and integration within the basin yields the population of 2.06 electrons for Li. The electron density distribution in the x,z plane and the cross-section of the zero-flux surface, D_d, are shown in Figure 1. Populations determined in this way will be called integrated Bader populations (IBP). Calculation of $P(x,z)$ with the same wave function, demarcation ($D_p(x,z)$, Fig. 2), and integration leads to the IPP value of 2.08 electrons of lithium. This IPP value is an approximation of IBP, for it contains two systematic errors.

The first error consists in the approximation of the rotationally symmetric zero-flux surface by a *vertical curtain*. This error will always increase the IPP value of the less polarizable atom compared to IBP (*vide infra*). Moreover, Figures 1 and 2 show that the critical point $(2,0)_p$ is moved toward Li with respect to the critical point $(3,-1)$. The difference in the relative positions of these bond critical points; 0.088 Å, can be used to characterize this error.[49] It also can be seen

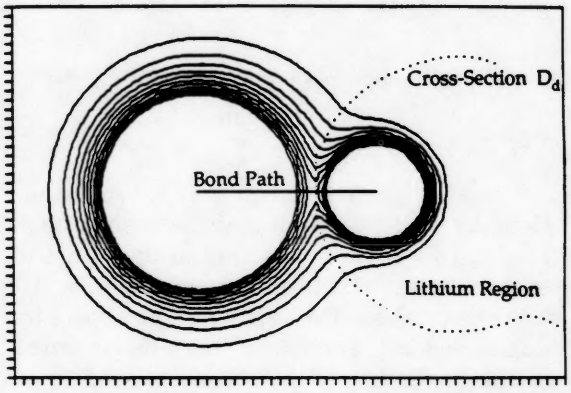

Figure 1. Contour map of the electron density of LiCl. Contours start at $0.005e$ *a.u.*$^{-3}$ with a level spacing of 0.005. Chlorine is located at the origin and lithium lies on the z axis, z = 2.072 Å. The bond path is shown as a solid line and the bond critical point occurs at z = 1.380 Å (MD 0.037). The cross-section of the zero-flux surface is shown as a dotted line.

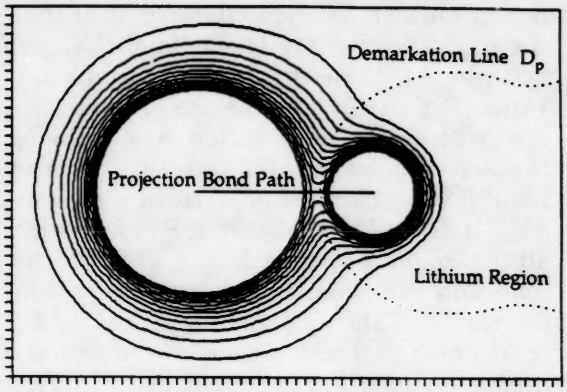

Figure 2. Contour map of the projection function of LiCl. Contours start at 0.01e $a.u.^{-2}$ with a level spacing of 0.01. The molecule is oriented as in Figure 1. The critical point along the projected bond path occurs at z = 1.468 Å (MPD 0.103). The demarcation line D_p is shown as a dotted line.

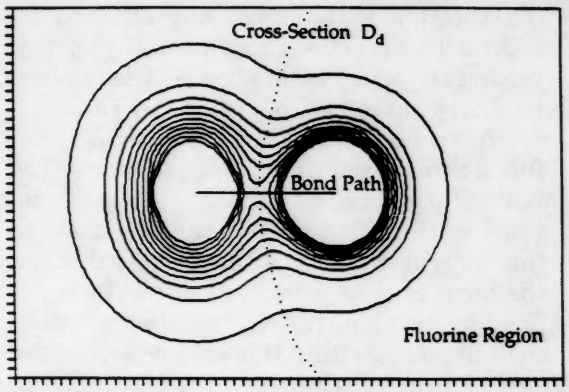

Figure 3. Contour map of the electron density of FCl. Contours start at 0.005e $a.u.^{-3}$ with a level spacing of 0.030. Chlorine is located at the origin and fluorine lies on the z axis, z = 1.613 Å. The bond path is shown as a solid line and the bond critical point occurs at z = 0.734 Å (MD 0.191). The cross-section of the zero-flux surface is shown as a dotted line.

that the line D_p (Fig. 2) engulfs the less polarizable atom more tightly than does the cross-section D_d(Fig. 1). The displacement of the bond critical points and the compression of the line D_p can be described in exact analogy (*vide infra*), and this second error needs to be accounted for by a second term in the difference between IPP and IBP. Both errors and the characteristic values that describe them become zero in the limiting case of a homonuclear diatomic molecule.

A large difference of the electronegativities of two connected atoms results in small values of $\rho(r)$ and $P(x, z)$ in the internuclear region ("ionic bonding") and the precise location of the partitioning surface is not as crucial. Such assumptions are no longer justified if the electronegativity difference is smaller. In FCl, for example, the displacement between D_p and D_d, Δ_{BCP} = 0.044 Å, is reduced (Figs. 3 and 4). Nonetheless, because of the increased electron density in the bonding region small differences in shape and location of the partitioning surface might affect significantly the integration result. Because the partitioning is the most crucial factor in the determination of populations, a quantitative comparison between projection populations IPP and the populations IBP is important. Here relations between IPP and IBP are derived for diatomic molecules A–B, where atom A is the less polarizable atom. LiCl and FCl typify limiting cases. Chlorine is atom B in LiCl and FCl. Note that Li and F are both less polarizable than Cl, although

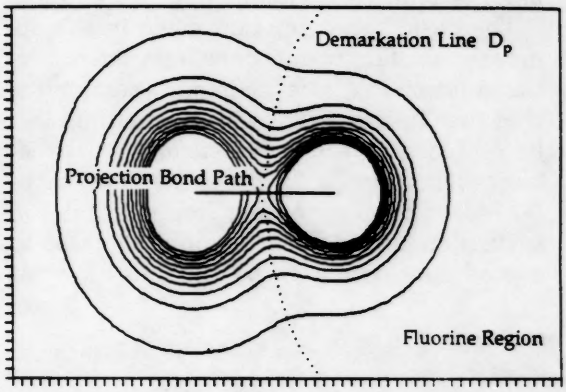

Figure 4. Contour map of the projection function of FCl. Contours start at 0.01e $a.u.^{-2}$ with a level spacing of 0.06. The molecule is oriented as in Figure 3 and the critical point along the projected bond path occurs at z = 0.778 Å (MPD 0.483). The demarcation line is shown as a dotted line.

atom A is positively charged for A = Li and negatively charged for A = F.

The geometric orientation was selected as follows: The internuclear axis of A–B coincides with the z axis. The right-handed Cartesian coordinate system originates at the bond critical point and A is placed on the negative z axis. Projections are parallel to the y axis.

Definition of the Polarization Volume and Its Components

The $C_{\infty v}$-symmetric zero-flux surface ZFS and its cross-sections with the xz plane

($D_d[x, z]$) and with the yz plane ($D_d[y, z]$), respectively, are shown schematically in Figure 5. The population of atom A is determined by integration of $\rho(r)$ within the $C_{\infty v}$-symmetric conical basin. It is useful to define a second conical volume as follows. The *natural partitioning*[18] plane $N_d(x, y)$ is defined as the plane that is perpendicular to the molecular axis and that passes through the bond critical point. A volume V_d is defined by the plane $N_d(x, y)$ and the condition that all points within this volume are on the side of atom A. The second conical volume can then be defined as the difference between V_d and the basin of atom A. The electron density contained in this second conical volume belongs to atom B, despite this volume's closer proximity to the atom A. This second conical volume will be called the *polarization volume*, PV_d. In the limiting case of a homonuclear diatomic PV_d will be zero.

The basic approximation made in the approach to obtain populations from the projection function $P(x, z)$ is the implicit assumption that the $C_{\infty v}$-symmetric zero-flux surface can be replaced by a *vertical curtain* in three-dimensional space. In the *ideal* case where $D_d = D_p$ this assumption implies that the surface engulfing atom A can be replaced to a good approximation by the only C_s-symmetric surface $S(x, y, z)$ defined such that the points $S(x, z)$ are elements of $D_d(x, z)$, and where the coordinate y can assume any value (Fig. 5). To describe the error associated with this approximation, a splitting of the *polarization volume* into two parts is helpful. The *vertical polarization volume* $PV_{d,v}$ is defined as that part of PV_d for which all the contained points $M(x, y, z)$ fulfill the condition that their projections are within the region of the xz plane demarked by D_d (x, z) around atom A. The *horizontal polarization volume* $PV_{d,h}$ is defined as the difference between the volumes PV_d and $PV_{d,v}$.

The definition of the *polarization volume* is based on the ZFS and the definitions of its vertical and horizontal components are based on the cross-section $D_d(x, z)$. Now, we need to consider the changes of the polarization volume that occur when the three-dimensional electron density is partitioned based on the demarcation line $D_p(x, z)$ of $P(x, z)$. In this case $S(x, y, z)$ is replaced by a surface $T(x, y, z)$ for which all the points $T(x, z)$ are elements of $D_p(x, z)$ and the y coordinate can assume any value. This surface and the plane N_p parallel to $N_d(x, y)$ and passing through the projection bond critical point define a volume that corresponds topologically to the horizontal polarization volume $PV_{d,h}$ and it will be

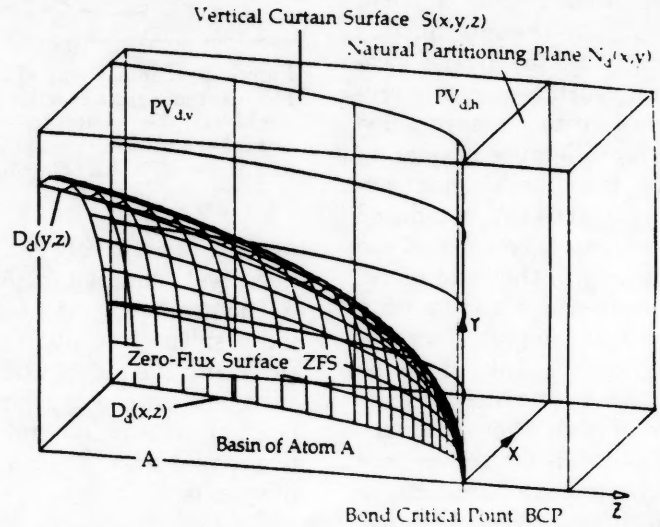

Figure 5. Schematic representation of the zero-flux surface of the gradient of the electron density, $\nabla\rho(x, y, z)$, of a diatomic molecule A–B, where A is the less polarizable atom. The natural partitioning plane $N_d(x, y)$ is orthogonal to the internuclear axis and contains the bond critical point BCP. The volume between $N_d(x, y)$ and the zero-flux surface is the polarization volume PV_d. The surface $S(x, y, z)$ defines the vertical and horizontal components of the polarization volume.

called the *horizontal projection polarization volume*, $PV_{p,h}$.

Relations Between Density Integration Populations

The first consideration is how IBP and IPP of atom A differ in the *ideal* case in which $D_p(x, z)$ and $D_d(x, z)$ are assumed to be identical and the effects of their difference are subsequently taken into account. In this *ideal* case $PV_{d,h}$ and $PV_{p,h}$ are identical, and the electrons in this common volume are assigned to the correct atom, B. However, the projection method falsely assigns the electron density contained in the *vertical polarization volume* $PV_{d,v}$ to atom A and causes the IPP(A) to be larger than IBP(A). Denoting the number of electrons in $PV_{d,v}$ as $E(PV_{d,v})$, the following relation is obtained between IBP and IPP of atom A (in the following all populations will refer to the atom A unless otherwise specified) in the *ideal* case, IPP_{id}:

$$IPP_{id} = IBP + E(PV_{d,v}) \qquad (1)$$

The next step examines how IPP_{id} deviates from IPP as a result of the nonequality of the demarcation lines D_d and D_p. In the following the three-dimensional electron density distribution is analyzed to ascertain why the lines D_d and D_p do not coincide and how they differ.

To evaluate the relation between the demarcation lines, a series of volume elements is considered that are defined by two planes, parallel to the yz plane with $x = +0.5\Delta$ and $x = -0.5\Delta$, respectively, and a series of planes $N_{p,n}(n = 0 \ldots n)$ that are parallel to the plane $N_p(x, y)$, separated by a distance Δ and intersecting the internuclear axis between the bond critical point and atom A. The first plane $N_{p,0}$ intersects the z axis at $z = 0.5\Delta$. The planes $N_{p,i}$ and $N_{p,i+1}$ define a volume element U_i with a squared face of lengths Δ and extending to infinity into both y directions. The zero-flux surface dissects these volume elements into two parts as illustrated schematically in Figure 6; the inner part U_i^{inner} containing electrons that belong to atom A and the outer part U_i^{outer} that contains electrons that belong to atom B. If Δ is selected sufficiently small, then the quotient between the number of electrons in the volume element U_i and the area element Δ^2 defines the value of $P(x, z)$ on the molecular axis at $z = -(i \cdot \Delta)$. In analogy the quotients between the numbers of electrons in the volumes U_i^{inner} and U_i^{outer}, respectively, and the area element Δ^2 define the contributions to the projection function arising from electron density of atom A, P_i^{inner}, and from atom B, P_i^{outer}. Considering the shape of the zero-flux surface it is almost trivial to state that P_0^{inner} is negligible at the bond critical point and that P_i^{inner} increases with increas-

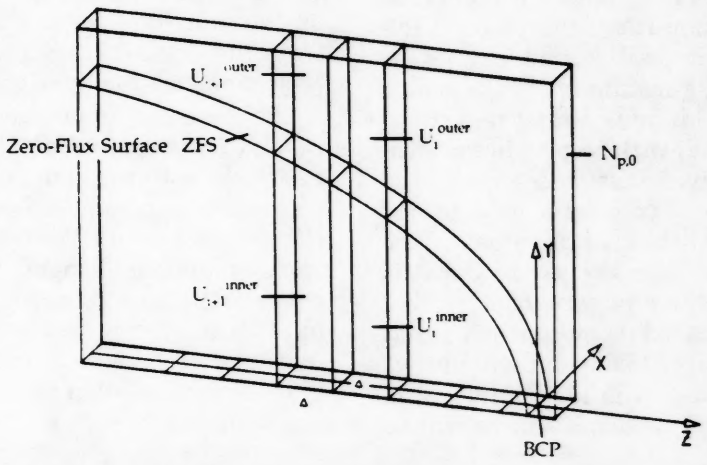

Figure 6. Schematic representation of the volume elements U_i. The *inner* and *outer* components of U_i result from dissection of U_i by the zero-flux surface. Half of the volume elements are shown (positive y).

ing i, while P_0^{outer} has a finite value and P_i^{outer} decreases with increasing i.

The incremental decrease of P_i^{outer} in going from volume element i to volume element $i + 1$ is given by

$$\Delta P_{i,i+1}{}^{\text{outer}} = -\Delta V \cdot \rho_i \qquad (2)$$

where ΔV equals $U_i^{\text{outer}} - U_{i+1}^{\text{outer}}$ and ρ_i is the average electron density in that volume of U_i^{outer} that is being lost. The corresponding incremental increase of P_i^{inner} is given by the similar expression

$$\Delta P_{i,i+1}^{\text{inner}} = \Delta V \cdot \rho_{i+1} \qquad (3)$$

where ρ_{i+1} is the average electron density in that part of $U_{i+1}{}^{\text{inner}}$ that is being gained.

Now suppose that ρ_i and ρ_{i+1} were related such that $\rho_i < \rho_{i+1}$ is true for *all* i. The increase $\Delta P_i^{\text{inner}}$ would be larger than the decrease $\Delta P_i{}^{\text{outer}}$ and P_i would increase constantly as i increases. This would lead to a negative slope of finite value of $P(0, z)$ at $z = \Delta$ and, hence, $P(0, \Delta)$ would have to be smaller than $P(0, 0)$. This case can only be realized if $\rho_t(0.5 \cdot \Delta)$ was smaller than $\rho_t(0)$ for some $t > t'$ ($t = x^2 + y^2$), since $\rho_{t=0}(0.5 \cdot \Delta)$ is, by definition of the bond path, larger than $\rho_{t=0}(0)$. It then follows that $\delta\rho_t(z)/\delta z$ would be negative for $t > t'$. This is impossible because the shape of the zero-flux surface allows only positive values of $\delta\rho(z)/\delta z$ for $z > 0$. The condition $\rho_{i+1} > \rho_i$ for *all* i has thus been proved wrong by contradiction. As the partial derivative of $P(0, z)$ with respect to the z coordinate at the bond critical point cannot be negative and because it could only be zero for a homonuclear diatomic, it follows that it has to be positive, that is $\rho_{i+1} < \rho_i$. Since P_i assumes a maximum at the center of atom A, it is obvious that the partial derivative of $P(0, z)$ with respect to the z coordinate is negative for some $i > i_{\text{critical}}$; the condition $\rho_i < \rho_{i+1}$ is true for some values of i but not for all. At the critical value of i the slope of $\delta P(0, z)/\delta z$ changes its sign; that is $z = -i \cdot \Delta$ marks the *projection bond critical point* (PBCP). It can thus be concluded that the projection bond critical point will always be displaced toward the less polarizable atom. The value of the displacement will be called Δ_{BCP}.

Consider now a similar set of volume elements V_j. The relation between the volume elements V_j and U_i is shown schematically in Figure 7. Each element V_j is contained between two planes that are parallel to each other, separated by Δ, perpendicular to the xz plane and follow the function $x_1 = f(z)$ and $x_2 = f(z)$. In addition the condition is imposed that atom A lies in the middle between these two planes. To complete the definition of the volume elements V_j the planes $M_{j,n}(n = 0 \ldots n)$ are defined that are perpendicular to the two previously defined planes and to the xz plane. In the special case of the functions $x = f(z)$ being simply $x_1 = 0.5 \cdot \Delta$ and $x_2 = -0.5 \cdot \Delta$, the volume elements V_j and U_i become identical. Analogous to the definition of U_0, the volume element V_0 is defined as that volume element that contains part of the demarcation line $D_d(x, z)$ in its basis area. For exactly the same reason which causes the position of the projected bond critical point to deviate from the position of the bond critical point of the electron density by Δ_{BCP}, *all* points of the demarcation line $D_d(x, z)$ are displaced by a value $\Delta_{1,f}$ (the index f indicates that $\Delta_{1,f}$ depends on the function $x = f(z)$) toward atom A to form the demarcation line $D_d(x, z)$ of the projection electron density function $P(x, z)$.

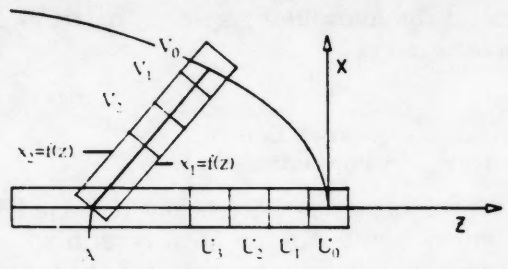

Figure 7. The basis areas of the volume elements U_i and V_j are shown in the xz plane illustrating the analogy between the volume elements.

The presented arguments relating the lines D_d and D_p show that *all* the points of $D_d(x, z)$ are shifted toward atom A along the line defined by each point of $D_d(x, z)$ and atom A. IPP deviates from IPP_{id} because all the electrons in volume elements U_i and V_i located between the lines D_d and D_p are not assigned to atom A, in contrast to the ideal case. If this amount of electrons is referred to as $E_{\Delta D}$, the following relation between IPP and IPP_{id} is obtained:

$$\text{IPP} = \text{IPP}_{id} - E_{\Delta D} \qquad (4)$$

Insertion of Eq. (4) into Eq. (1) yields the relation between IPP and IBP:

$$\text{IPP} = \text{IBP} + E(PV_{d,v}) - E_{\Delta D} \qquad (5)$$

Limiting Cases

To compare the values of the projection population with IBP in dependence of the bond polarity the term ΔP

$$\Delta P = E(PV_{d,v}) - E_{\Delta D} \qquad (6)$$

needs to be examined. Equation (6) is first examined with regard to the sign of ΔP and values of ΔP, $E(PV_{d,v})$ and $E_{\Delta D}$ are discussed later.

The zero-flux surface dissects the volume $V_{\Delta D}$ into an inner and an outer component. The numbers of electrons contained in these components of $V_{\Delta D}$ will be called $E_{\Delta D}^{\text{inner}}$ and $E_{\Delta D}^{\text{outer}}$, respectively. $E_{\Delta D}$ is simply the sum of its two components:

$$E_{\Delta D}^{\text{inner}} + E_{\Delta D}^{\text{outer}} = E_{\Delta D} \qquad (7)$$

$\Delta PV_{d,v}$ is defined as that part of the vertical polarization volume that remains after subtraction of the volume common to $PV_{d,v}$ and $V_{\Delta D}$ and the number of electrons in $\Delta PV_{d,v}$ is denoted as $E(\Delta PV_{d,v})$. $E(PV_{d,v})$ is related with $E(\Delta PV_{d,v})$ by

$$E(\Delta PV_{d,v}) + E_{\Delta D}^{\text{outer}} = E(PV_{d,v}) \qquad (8)$$

Introduction of Eqs. (7) and (8) into Eq. (6) yields for ΔP

$$\Delta P = E(\Delta PV_{d,v}) - E_{\Delta D}^{\text{inner}} \qquad (9)$$

With Eq. (9) two cases may be differentiated. For the limiting case of a bond between atoms with a small electronegativity difference (low bond polarity) the relation

$$E_{\Delta D}^{\text{inner}} > E(\Delta PV_{d,v}) \qquad (10a)$$

should hold since all points in the volume $\Delta PV_{d,v}$ are in a region of low electron density whereas the electron density is comparatively higher at all points in $V_{\Delta D}^{\text{inner}}$. ΔP becomes negative in this case. Considering Eq. (5), Eq. (10a) can be rewritten as

$$\text{IPP} < \text{IBP}; \qquad \text{limit I} \qquad (10b)$$

In this case, limit I, the IPP value of the less polarizable atom is smaller than IBP.

The reverse of relation (10a), namely

$$E_{\Delta D}^{\text{inner}} < E(\Delta PV_{d,v}) \qquad (11a)$$

can be realized for highly polar systems. Again, relation (11a) can be restated using Eq. (5) as

$$\text{IPP} > \text{IBP}, \qquad \text{limit II} \qquad (11b)$$

and the conclusion is reached that *the IPP value of the less polarizable atom of a highly polar diatomic is larger than IBP.*

Depending on the polarity of the bonding, the IPP value of the less polarizable atom can either be smaller (limit I) or larger (limit II) than IBP, and IPP may become incidently identical with IBP by cancellation of the terms $E_{\Delta D}^{\text{inner}}$ and $E(\Delta PV_{d,v})$. If it were possible to classify bonds as belonging to one of these two limiting cases (*vide infra*) the sign of ΔP would allow an important statement as to whether IPP is larger or smaller than IBP. Moreover, this analysis suggests an alternative mode of demarking $P(x, z)$ that allows for the determination of the maximum error associated with the projection population of atoms in bonding situations that follow limit I. The primary role in this discussion falls to IPP_{id}.

A New Projection Population: IPP2

Introduction of Eq. (1) into Eq. (10b) gives the relation

$$\text{IPP} < \text{IBP} < \text{IPP}_{id}; \qquad \text{limit I} \qquad (12)$$

and introduction of Eq. (4) into Eq. (11b) gives the corresponding relation for limit II:

$$\text{IBP} < \text{IPP} < \text{IPP}_{id}; \qquad \text{limit II} \qquad (13)$$

These two relations allow for several conclusions. First, for *any* diatomic molecule IBP of the less polarizable atom will always be *smaller* than IPP_{id}; IPP_{id} thus defines an *upper limit* of the population of atom A. A similar relation does not hold for IPP. Second, if the bond polarity is such that relation (12) is valid, then IBP falls between the two projection populations. IPP and IPP_{id} thus determine the *lower and the upper limits* to IBP.

In addition, the arguments presented suggest that IPP_{id} will be a better approximation to IBP than IPP in the partitioning of bonds belonging to the case typified by limit I. IPP is too small compared to IBP by $E_{\Delta D}^{\text{inner}} - E(\Delta PV_{d,v})$, and IPP_{id} is too large compared to IBP by $E_{\Delta D}^{\text{outer}} + E(\Delta PV_{d,v})$. If the curvature of the zero-flux surface becomes rather small, which happens in strongly bonded systems with low bond polarities (*vide infra*), then $E(\Delta PV_{d,v})$ becomes negligible and IPP (IPP_{id}) will approximately be too small (large) by $E_{\Delta D}^{\text{inner}}$ ($E_{\Delta D}^{\text{outer}}$) compared to IBP. Since $E_{\Delta D}^{\text{inner}} >> E_{\Delta D}^{\text{outer}}$, it then follows that IPP_{id}

has to be the better approximation to IBP. This conclusion can be reached qualitatively from a probably more familiar perspective. Consider the projection functions of the π_{oop}- and the (ρ-π_{oop}) electron densities. The π_{oop} density incorporates the contributions to $\rho(r)$ associated with π_{yz} MOs and the (ρ-π_{oop}) density incorporates all others.[50] Since polarization of the σ density is comparatively small and because the in-plane π MOs have no density along the bond, the bond critical point and the projection bond critical point of the (ρ-π_{oop})-density will coincide to a very good approximation. It is then the projection of the π_{oop} electron density that is primarily responsible for the deviation between the critical points BCP and PBCP as a result of polarization of the π_{oop} density toward the less polarizable atom. The use of $D_d(x, z)$ will assign too much of the projected π_{oop} density to atom A, whereas the use of $D_p(x, z)$ will assign too little of the (ρ-π_{oop}) density to atom A. In bonds of low polarity, the magnitude of the projected (ρ-π_{oop}) density is much larger than is the magnitude of the projected π_{oop} density. For example, the values of the projected (ρ-π_{oop}) and the π_{oop} densities, respectively, calculated at 6–31G* for N_2 and for ethine are as follows (in e a.u.$^{-2}$): 0.93 and 0.31 for N_2; and 0.67 and 0.24 for ethine. The σ-density accounts for about 75% of the projected total density in these molecules. In systems with low bond polarities it thus appears more important to approximate the partitioning of the projected (ρ-π_{oop}) density in the best possible way, than it is to partition the π_{oop} density in the best possible way.

The recognition of IPP_{id} as an important parameter suggests that the integration of $P(x, z)$ be performed in two ways. Aside from the determination of IPP by use $D_p(x, z)$, it is suggested to integrate $P(x, z)$ using the cross-section $D_d(x, z)$ as a boundary line to determine IPP_{id}. It is suggested to refer to IPP_{id} as IPP2. The index "ideal" is self-explained in the present context. Taken out of this context, however, the index may lead to unwarranted implications as to the accuracy of the value.

APPLICATIONS

Computational Aspects

Wavefunctions were calculated with the program GAUSSIAN82.[51] The 6-31G* basis set[52] was used for the diatomic molecules and the 3-21+G basis set[53] was used for the anions. Structures were optimized or taken from the literature.[39,54,55] Projection functions and cross-sections of $\rho(r)$ were calculated with the program PROJ by Collins et al. and others[34–36] with the usual grid spacing of 0.2 a.u. Contour maps were generated and the program DEMARK written by McDowell et al.[37] was used for the determination of the boundary lines D_p for $P(x, z)$ and D_d for $\rho(r)$ and for the integration of $P(x, z)$ within the closed regions demarked by D_p and D_d to determine the projection populations IPP and IPP2, respectively. Bond properties were determined with Biegler-König's program EXTREME[56] and atomic properties were calculated with the program PROAIMS written by Biegler-König and Duke.[57] Most calculations were carried out on a VAX-11/750 computer and MicroVax II computers and workstations. Atomic properties were computed with a CSPI Maxim-64 array rocessor hosted by a MicroVax II system.

The locations of the projection bond critical points and of the bond critical points determined from the grid data obtained with PROJ are given by the parameter F and F2, respectively. F (F2) is defined for the bond A—B as the fraction of the distance between atom A and the PBCP (BCP) with respect to the bond length d(A—B). F and F2 were calculated, to a good approximation, assuming linear (projection) bond paths. Bond properties determined with EXTREME were characterized by the values r_A, r_B, and F3. The value of r_A (r_B) gives the distances of atom A (B) from the bond critical point of the AB bond in angstroms. The parameter F3 is analogous to the F2 value; different names are used because the F3 values were determined by a Newton-Raphson walk, whereas the F2 values were determined by least-squares fit procedures of grid data.[37] The agreement between the F2 and the F3 value is satisfactory (*vide infra*) and Δ_{BCP} values given are based on the F2 values. The values MPD and MD are the minimum values along the projection bond path and along the bond path, respectively. MD values determined from the grid data produced with PROJ and EXTREME are virtually the same. Critical points were characterized by their eigenvalues λ_i of the Hessian matrix of $\rho(r)$, by the values of the Laplacian of the

density $\nabla^2(\rho)$ and by the bond ellipticities ε.[23,27] Kinetic energies of the atoms, T′ and T″ (corrected for the virial defect of the wavefunction), the deviations between the sum of the integrated kinetic energies of the atoms and kinetic energy of the molecule, and the L values are reported to characterize the accuracy of the integrations.

Diatomic Molecules

Pertinent results are summarized in Table I. Bond properties and further results of the three-dimensional integrations are given in tables in supplemental material (see Ref. 60), and will be discussed elsewhere. Contour maps of $P(x,z)$ and of cross-sections of $\rho(r)$ containing the appropriate demarcation lines can be obtained from the author.

The demarcation lines D_p are displaced toward the less polarizable atom compared to D_d; F2 is larger than F in all cases. The Δ_{BCP} values (Table II) are generally between 0.01 and 0.10 Å. Relative displacements are generally 5% or less, but larger deviations are

Table I. Electron density analysis of diatomic molecules.[a–e]

AB	d(AB)	MP	IBP	F	MPD	IPP	F2	MD	IPP2
LiF	1.555	2.339	2.054	0.39	0.159	2.088	0.40	0.076	2.114
LiCl	2.072	2.498	2.059	0.29	0.103	2.084	0.33	0.037	2.128
NaF	1.885	10.296	10.069	0.44	0.135	10.073	0.49	0.060	10.116
NaCl	2.393	10.332	10.081	0.39	0.091	10.097	0.43	0.031	10.139
BeO	1.296	3.596	2.268	0.32	0.434	2.450	0.35	0.195	2.530
BeS	1.733	3.653	2.372	0.31	0.311	2.597	0.32	0.101	2.705
MgO	1.739	11.185	10.689	0.43	0.226	10.719	0.47	0.084	10.756
MgS	2.149	11.538	10.672	0.39	0.190	10.749	0.40	0.055	10.832
BN	1.239	4.690	3.344	0.34	0.619	3.643	0.34	0.229	3.767
BP	1.637	4.152	5.551	0.52	0.463	5.270	0.58	0.128	5.558
CO[f]	1.114	5.732	4.595	0.29	0.905	4.753	0.39	0.491	4.951
CS	1.520	6.032	6.873	0.50	0.720	6.170	0.62	0.266	6.899
SiO	1.487	13.350	12.437	0.42	0.461	12.569	0.43	0.188	12.640
SiS	1.917	13.605	12.706	0.33	0.375	12.756	0.39	0.123	12.871
PN	1.455	14.591	13.403	0.42	0.633	13.629	0.42	0.240	13.676
FCl	1.613	9.363	9.501	0.52	0.483	9.428	0.54	0.191	9.571

[a] $^1\Sigma^+$ States calculated at RHF/6-31G*.
[b] The minimum value MD (MPD) of the electron density (projection function) along the bond is given in e a.u.$^{-3}$ (e a.u.$^{-2}$).
[c] Bond lengths d(AB) in Å. The distance of the bond critical point PBCP (BCP) from atom Å is given by the fraction F (F2) of the bond length d(AB).
[d] Values of IBP, IPP, IPP2, and of Mulliken populations (MP) are given for the less polarizable atom in electrons.
[e] Most structures taken from Ref. 54.
[f] At RHF/6-31G** a charge of +1.4 was reported for carbon in CO, cf. Ref. 28d.

Table II. Comparison of integrated populations IPP, IPP2, and IBP. Diatomic molecules.

Atom	$E(PV_{d,v})$ IPP2-IBP	$E_{\Delta D}$ IPP2-IPP	ΔP IPP-IBP	Δ_{BCP}
LiF: Li	0.060	0.026	0.034	0.013
LiCl: Li	0.069	0.044	0.025	0.088
NaF: Na	0.047	0.043	0.004	0.097
NaCl: Na	0.058	0.042	0.016	0.098
BeO: Be	0.268	0.080	0.182	0.036
BeS: Be	0.333	0.108	0.225	0.012
MgO: Mg	0.067	0.037	0.030	0.073
MgS: Mg	0.160	0.083	0.077	0.021
BN: B	0.423	0.124	0.299	0.005
BP: B	0.007	0.288	−0.281	0.097
CO: C	0.356	0.198	0.158	0.109
CS: C	0.026	0.729	−0.703	0.195
SiO: Si	0.203	0.071	0.132	0.012
SiS: Si	0.165	0.115	0.050	0.110
PN: P	0.273	0.047	0.226	0.011
FCl: F	0.070	0.143	−0.073	0.044

found for CO (10%) and CS (12%, Δ_{BCP} = 0.20 Å). No significant correlations are found between the absolute or the relative displacements and parameters that reflect the bond polarity.

The halides of the alkali metals are what one might call typical ionic molecules.[58] For these molecules, relation 13 should hold and the data in Table II show this to be true. IPP and IPP2 overestimate the metal population by ΔP and $E(PV_{d,v})$, respectively, and IPP2 deviates more from IBP than does IPP. The vertical polarization volume of LiCl, for example, contains $E(PV_{d,v})$ = 0.07 electrons which are falsely assigned to Li if the vertical curtain-type partitioning defined by D_d is used. Integration of $P(x,z)$ using D_p reduces the error caused by $PV_{d,v}$ by $E_{\Delta D}$ = 0.04 electrons and IPP deviates ΔP = 0.03 electrons from IBP. The values of ΔP and of $E(PV_{d,v})$ are rather small for the halides and projection populations are excellent approximations to IBP.

All other molecules have more shared electron density than the alkaline halides. The values of MD and MPD are increased and/or the lines D_d (and D_p) engulf atom A less tightly. For example, IBP(Be) for BeO is 2.27 electrons resulting in a charge of +1.73 for Be. IPP and IPP2 are 2.45 and 2.53 electrons, respectively, and relation 13 applies. $E(PV_{d,v})$ is 0.27 for BeO; about fourfold larger than for the halides. Demarcation of $P(x,z)$ using D_p reduces the deviation from IBP by $E_{\Delta D}$ = 0.08, but IPP remains 0.18 too high. The IBP value of boron in BN shows a charge of +1.66; indicating comparable charge transfer in BN and BeO. The triple-bonded nitride BN shows the largest value of $E(PV_{d,v})$ of the diatomics, 0.42 electrons (Table II and table in supplemental material, Ref. 60). The critical points of $P(x,z)$ and of $\rho(r)$ of BN are displaced slightly, but D_d and D_p differ away from the internuclear axis. The differences between D_p and D_d result in an IPP of 3.64 electrons; still 0.31 larger than IBP. As with BeO and BN, significantly overestimated IPP and IPP2 values are found (Table II) and for all of these molecules, except BP, CS, and FCl, relation 13 applies, that is IBP < IPP < IPP2.

The molecules BP, CS, and FCl satisfy relation 12, that is IPP < IBP < IPP2 for the less polarizable atom. Note that the less polarizable atoms in these molecules are negatively charged (A is electron deficient in all of the other diatomics); the IBP values are 5.55 (B), 6.87 (C), and 9.50 (F) electrons, respectively. The *π- and σ*-withdrawing ability of the less polarizable atoms is reflected in the F values; the basins of the less polarizable atoms extend over more than 55% of the bond in these cases; even so the more polarizable atom is a second-row atom. As always, IPP2 overestimates the population of the less polarizable bonding partner, but the $E(PV_{d,v})$ values are comparatively small (0.01 (BP), 0.03 (CS), and 0.07 (FCl) electrons). In contrast to the other diatomics, the $E_{\Delta D}$ values are larger than the $E(PV_{d,v})$ values, and the IPP values are smaller than the IBP values by 0.28 and 0.07 electrons for BP and FCl, respectively. CS stands out with an immense $E_{\Delta D}$ value of 0.73 electrons and a ΔP value of 0.70 electrons. A plot of a cross-section of $\rho(x,z)$ of the CS bond shows a wide range between the atoms with high electron density and with a small gradient of the electron density. For this type of bonding situation it has been argued above that IPP2 should be closer to IBP than IPP. The results for BN, CS, and FCl confirm this argument.[59]

Three distinct shapes of the demarcations lines (D_d or D_p) are found. Large curvatures are found for highly polar molecules and small curvatures are found for molecules with a comparatively little charge transfer, and the lines show a steady increase in curvature with distance from the internuclear axis. Semipolar molecules form the third group (e.g., BN, CO, SiO, SiS, and PN). For these molecules the part of the demarcation line in the vicinity of the internuclear axis is distinctly curved and, moreover, significantly more curved than the parts of D_d that are farther away. In other words, extrapolation of those parts of the demarcation line that are farther away from the axis (>0.2–0.3 Å) would intersect the axis between atom A and the bond critical point. Such a shape of D_d necessarily causes an increase of $PV_{d,v}$, and ΔP in turn, compared to molecules with smooth demarcation lines.

Polyatomic π-Conjugated Anions

The approximations intrinsic to projection populations might be discussed for more complex planar molecules in a similar fash-

ion as for the diatomics. The partitioning of a bond to a terminal fragment could be discussed in analogy, and for fragments within the molecular skeleton the effects of the approximative partitioning of several bonds would have to be examined. In contrast to the diatomic molecules the zero-flux surfaces of planar molecules are only C_s symmetric. The reduced symmetry does not affect the validity of any of the equations because all of the above considerations require only the point group C_s to be a subgroup of the symmetry point group of the molecule. The vertical polarization volume, the key element of the discussion, has been introduced as a part of the polarization volume. The polarization volumes of fragments cannot be defined in analogy to the diatomic molecules because of the shape of $D_d(x,z)$. However, without any loss in logic it can be abstracted from the way the vertical polarization volume was introduced to the way it is defined, namely as the volume contained between the zero-flux surface and the vertical curtain surface $S(x,y,z)$ for which all $S(x,z)$ are elements of $D_d(x,z)$. If, in addition, the surface $S(x,y,z)$ and the corresponding surface $T(x,y,z)$—a vertical curtain defined by $D_p(x,z)$—don't cross, then all the above considerations remain valid.

Here some π-conjugated anions are considered. The electronic structures of the anion of acetaldehyde (1), of the isomeric carbanions of ethylimine (*syn*-2 and *anti*-3), of allyl anion (4), and of the isomeric carbanions of acetaldoxime (*syn*-5 and *anti*-6), have been analyzed. The contour map of the cross-section of the electron density of 1 in the molecular plane (*xz* plane) is shown on top in Figure 8.[60] Some geometries were reported recently[55] and the others[61] are given in Ref. 60. The study of the electronic structures of these molecules is important for the understanding of CC bond-forming reactions.[39,55] A more detailed analysis of the bond properties (supplementary table), atomic properties of 1–6 other than population (supplementary table) and chemical implications will be presented elsewhere. Results pertinent to the present discussion are summarized in Tables III, IV, and V.

The positively charged CH group is the less polarizable bonding partner in both of the bonds X—$CHCH_2$ (X = O, NH, or NOH) and CH_2—CHX. The projection bond critical points of the CC and the CX bonds all are displaced toward the CH carbon compared to the bond critical points. The displacements (Table III) are comparable to those found for the diatomics.

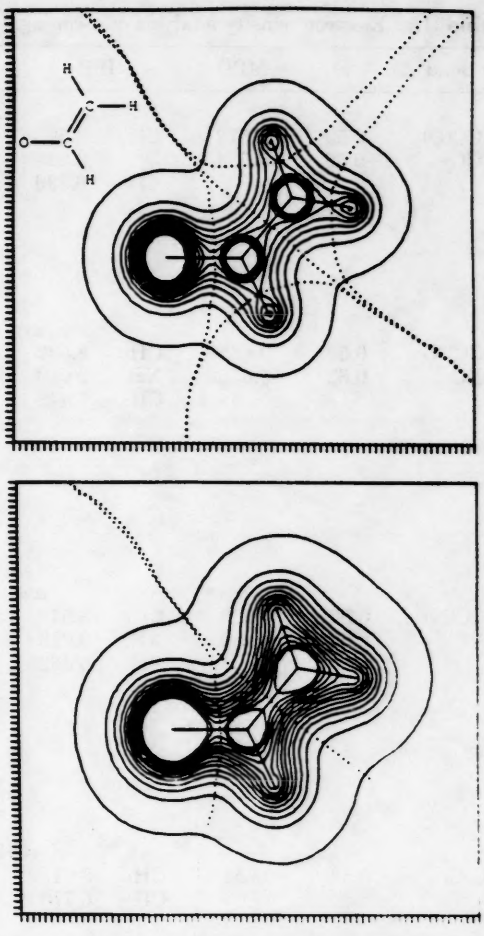

Figure 8. The cross-section of the electron density in the molecular plane (top) and of the projection function $P(x, z)$ of the enolate ion of acetaldehyde, 1. Contour levels are from 0.005 to 0.705 with a level spacing of 0.05*e* a.u.$^{-3}$ for $\rho(x, z)$ and from 0.005 to 0.705 with a level spacing of 0.05*e* a.u.$^{-2}$ for $P(x, z)$.

The Δ_{BCP} values are largest for the CC bonds. The IBP values (Table III) indicate charges ranging from −0.24 (5) to −0.43 (2) for the CH_2 fragments, and they indicate CH charges in the range between +0.30 (5) and +0.52 (1) for the heteroallylic anions, but a charge of −0.16 for allyl anion. All of the CC bonds are moderately polar with populations differences between the bonded fragments of 0.26 for 4 and of about 0.55–0.85 for the other anions. As with the diatomic molecules with low bond polarities, relation 12 applies to the CC bonds. Since the CH_2 group is the

Table III. Electron density analysis of π-conjugated anions.[a-c]

Bond	F	MPD	IPP		Bond	F2	MD	IPP2		IBP
					CH_2CHO^-, 1					
CC(O)	0.53	0.672	CH_2	8.523	CC(O)	0.44	0.308	CH_2	8.240	8.357
OC	0.65	0.634	O	9.238	OC	0.63	0.319	O	9.257	9.166
			CH	6.239				CH	6.503	6.477
					CH_s	0.61	0.257	H_s	1.173	1.028
					CH_a	0.64	0.256	H_a	1.174	1.059
					CH_c	0.63	0.258	H_c	1.155	1.075
								C(C)	5.893	6.270
								C(O)	5.348	5.402
					syn-CH_2CHNH^-, 2					
CC(N)	0.53	0.655	CH_2	8.532	CC(N)	0.47	0.294	CH_2	8.369	8.427
NC	0.63	0.655	NH	9.019	NC	0.58	0.317	NH	8.931	8.952
			CH	6.449				CH	6.700	6.624
					NH	0.68	0.306	H_n	0.864	0.774
					CH_s	0.64	0.252	H_s	1.188	1.056
					CH_a	0.64	0.253	H_a	1.186	1.057
					CH_c	0.62	0.261	H_c	1.107	1.042
								N	8.067	8.178
								C(C)	5.995	6.314
								C(N)	5.593	5.582
					anti-CH_2CHNH^-, 3					
CC(N)	0.50	0.668	CH_2	8.519	CC(N)	0.45	0.302	CH_2	8.299	8.356
NC	0.63	0.650	NH	9.020	NC	0.58	0.314	NH	8.939	8.951
			CH	6.462				CH	6.762	6.692
					NH	0.64	0.309	H_n	0.891	0.781
					CH_s	0.60	0.257	H_s	1.166	1.026
					CH_a	0.63	0.254	H_a	1.225	1.067
					CH_c	0.65	0.254	H_c	1.141	1.077
								N	8.048	8.170
								C(C)	5.908	6.262
								C(N)	5.621	5.615
					$CH_2CHCH_2^-$, 4[d]					
C_tC_c	0.53	0.651	CH_2	8.615	C_tC_c	0.45	0.292	CH_2	8.325	8.419
			CH	6.770				CH	7.350	6.692
					CH_s	0.59	0.254	H_s	1.227	1.056
					CH_a	0.57	0.253	H_a	1.261	1.069
					CH	0.62	0.257	H	1.155	1.056
								C_t	5.837	6.294
								C_c	6.195	6.108
					syn-CH_2CHNOH^-, 5					
CC(N)	0.50	0.673	CH_2	8.419	CC(N)	0.45	0.302	CH_2	8.200	8.242
NC	0.63	0.654	NOH	17.129	NC	0.62	0.318	NOH	17.120	17.067
NO	0.50	0.438	OH	9.351	NO	0.42	0.199	OH	9.428	9.385
			CH	6.453				CH	6.680	6.691
			N	7.778				N	7.696	7.682
					OH	0.74	0.335	H_o	0.686	0.554
					CH_s	0.60	0.263	H_s	1.150	0.986
					CH_a	0.63	0.256	H_a	1.200	1.060
					CH_c	0.60	0.266	H_c	1.110	1.021
								O	8.742	8.831
								C(C)	5.850	6.196
								C(N)	5.570	5.670

(cont.)

more polarizable bonding partner, relation 12 implies the ordering IPP > IBP > IPP2 for the CH_2 populations. The absolute deviations between IPP and IBP are larger than between IPP2 and IBP (Table IV).

The populations indicate that the negative charge is localized, to a great extent, on the heteroatom (Table III). The CX bonds have charge differences in excess of 1.25 between 1.25 between the bonded fragments. The lowest bond polarities are found for 2 and 3, and relation 12 applies in its formulation for the more polarizable bonding partner, IPP2 < IBP < IPP. The populations of 1, 5, and 6 show the limitations imposed on the systematic evaluation of the approximations of IPP and IPP2 of polyatomic molecules by the complexity of the zero-flux surface. For 1

Table III. (continued)

Bond	F	MPD	IPP	Bond	F2	MD	IPP2	IBP
			anti-CH_2CHNOH^-, 6					
CC(N)	0.53	0.668	CH_2 8.456	CC(N)	0.44	0.299	CH_2 8.206	8.293
NC	0.64	0.652	NOH 17.124	NC	0.65	0.318	NOH 17.108	17.066
NO	0.48	0.420	OH 9.376	NO	0.42	0.187	OH 9.462	9.405
			CH 6.420				CH 6.687	6.638
			N 7.748				N 7.646	7.661
				OH	0.79	0.335	H_o 0.620	0.551
				CH_s	0.59	0.255	H_s 1.190	1.027
				CH_a	0.64	0.258	H_a 1.158	1.048
				CH_c	0.63	0.267	H_c 1.056	0.975
							O 8.842	8.855
							C(C) 5.858	6.219
							C(N) 5.631	5.663

[a] Calculations are at RHF/3-21+G.
[b] See Table I, (b–d).
[c] *Syn* or *anti* denote a *cis* or *trans* relation, respectively, between the CH_2 and the E groups (E = H, OH) at N. H_c is connected to the C-atom that is bonded to X (X = O, NH, NOH). H_s (H_a) is the CH_2 hydrogen that is *syn*- (*anti*-) oriented with respect to X. H_o (H_n) is bonded to O (N).
[d] C_t (C_c) is the terminal (central) C-atom of allyl anion.
[e] Compare Ref. 62.

Table IV. Comparison of integrated populations IPP, IPP2, and IBP. π-conjugated anions.

Group	$E(PV_{d,v})$ IPP2–IBP	$E_{\Delta D}$ IPP2–IPP	ΔP IPP–IBP	$E(PV_{d,v})$ IPP2–IBP	$E_{\Delta D}$ IPP2–IPP	ΔP IPP–IBP
		CH_2CHO^-, 1				
CH_2	−0.117	−0.283	0.166			
CH	0.091	0.264	−0.238			
O	0.026	0.019	0.072			
		syn-CH_2CHNH^-, 2			*anti*-CH_2CHNH^-, 3	
CH_2	−0.058	−0.163	0.105	−0.057	−0.220	0.163
CH	0.076	0.251	−0.175	0.070	0.300	−0.230
NH	−0.021	−0.088	0.067	−0.012	−0.081	0.069
		$CH_2CHCH_2^-$, 4				
CH_2	−0.094	−0.290	0.196			
CH	0.186	0.580	−0.394			
		syn-CH_2CHNOH^-, 5			*anti*-CH_2CHNOH^-, 6	
CH_2	−0.042	−0.219	0.177	−0.087	−0.250	0.163
CH	−0.011	0.227	−0.238	0.049	0.267	−0.218
NOH	0.053	−0.009	0.062	0.042	−0.016	0.058
OH	0.043	0.077	−0.034	0.057	0.086	−0.029
N	0.014	0.082	0.096	−0.015	−0.102	0.087

Table V. Comparison of integrated populations of π-conjugated anions. $E(PV_{d,v})$ Values of hydrogens and atoms bonded to hydrogen(s).

Atom	1	2	3	4	5	6
C(C)	−0.377	−0.319	−0.354	−0.457	−0.346	−0.361
C(X)	−0.054	0.011	−0.006	0.087	−0.100	−0.032
H_s	0.145	0.132	0.140	0.171	0.164	0.163
H_a	0.115	0.129	0.158	0.192	0.140	0.110
H_c	0.080	0.065	0.064	0.099	0.089	0.081
N		−0.111	−0.122			
H_n		0.090	0.110			
O					−0.089	−0.013
H_o					0.132	0.069

[a] CH_2CHX^- with X = O, NH, NOH, and CH_2.
[b] See Table III, c.

$E(PV_{d,v})$, $E_{\Delta D}$, and ΔP all are positive. The ordering of the O populations is IPP2 > IPP > IBP, although D_p is displaced toward the CH carbon with respect to D_d. IPP2 is larger than IPP by $E_{\Delta D} = 0.02$ because the surfaces $S(x,y,z)$ and $T(x,y,z)$ between oxygen and the vinyl group cross. In the case of the oxime anions $E(PV_{d,v})$ and ΔP are positive while the $E_{\Delta D}$ values are negative. Neither relation 12 nor relation 13 apply here and the reasons for the deviations between the integrated populations remain obscured. In any case, the comparison of the values of $E(PV_{d,v})$ and ΔP reveals demarcations of $P(x,z)$ with D_d result in X populations that are in better agreement with IBP than are the IPP values.

Polarization causes significant positive charges of the central CH groups (*vide supra*). IPP greatly overestimates this electron depletion since IPP(CH) contains some contamination from the *vertical polarization volumes* of the X and of the CH_2 groups. The electron density in $PV_{d,v}$ causes the demarcation line to be shifted toward the CH carbon and causes the neglect of σ-density in IPP(CH). The populations of the CH groups illustrate the important point that, by using IPP2 instead of IPP, a better assignment of the σ-density is assured.

A final aspect concerns projection H populations. The regions between hydrogen and first-row elements usually contain no projection bond critical point, that is, demarcation lines D_p are not defined. In contrast, the cross-sections of $\rho(r)$ show well-defined valleys and IPP2 values can be determined as *upper limits* of the H populations. The differences $E(PV_{d,v})$ between the IPP2 and the IBP values of the H atoms in 1–6 are listed in Table V. The $E(PV_{d,v})$ values are comparable to the respective values for fragment populations, but the relative error is larger, and IPP2 values of hydrogens that are connected to first-row atoms therefore have little significance. Consequently, projection populations of atoms that are bonded to hydrogens are also of limited value (Table V). Projection populations of hydrogen atoms that are bonded to second-row atoms are more meaningful. Minima of $P(x,z)$ exist along the projected bond paths in these cases, and the populations are affected less by the electron density in the vertical polarization volume.[63,64]

SUMMARY AND CONCLUSION

The differences between projection populations and the populations determined by integration over basins have been analyzed for diatomic molecules using the properties of the zero-flux surfaces. The derived relations can be applied to polyatomic planar molecules. Deviations between IPP and IBP are attributed to two systematic errors. The first of these is intrinsic to projection techniques and consists in the replacement of the three-dimensional zero-flux surface by a vertical curtain-type surface. The second error relates to the inequality of the demarcation line D_p of the projection function and the cross-section D_d of $\rho(r)$. This error can be minimized in some cases if D_d is used instead of D_p to obtain the newly introduced projection population IPP2. It has been shown that the IPP2 value of the less polarizable atom is larger than IBP by the number of electrons in the vertical polarization volume, $E(PV_{d,v})$. The projection of the electron density causes a shift of all points of D_d toward the less polarizable atom. As a result, IPP is smaller than IPP2 by the term $E_{\Delta D}$, and IPP and IBP differ by $\Delta P = E(PV_{d,v}) - E_{\Delta D}$. $E_{\Delta D}$ can be smaller or larger in absolute value than $E(PV_{d,v})$ and two limiting cases have to be considered. For the populations of the less polarizable atom, the relation 12, IPP < IBP < IPP2, holds in the limiting case where $\Delta P < 0$, and the relation 13, IBP < IPP < IPP2, holds if $\Delta P > 0$. The physical significance of the values $E(PV_{d,v})$ and $E_{\Delta D}$ may be obscured in polyatomic planar molecules due to increased complexity of the zero-flux surfaces of $\nabla\rho(r)$. In these cases $E(PV_{d,v})$, $E_{\Delta D}$, and ΔP provide only numerical differences between the populations. Conclusions of the analysis have been tested and confirmed by calculations of populations for diatomic molecules and for simple polyatomic anions. For *any* diatomic molecule the population IBP of the less polarizable atom will always be *smaller* than the value of IPP2, that is, IPP2 determines an *upper limit* to IBP of the less polarizable atom. For bonds with low bond polarities relation 12 applies and IBP falls between the two projection populations, that is, IPP and IPP2 define the *maximal error* associated with the projection populations. IPP provides an excellent approximation for highly polar sys-

tems; IPP2 provides a better and equally satisfying approximation for systems of low bond polarity. In the intermediate semipolar bonding situations the deviations between the projection populations and IBP may exceed 0.1 electrons. Such bonding situations can usually be identified by the shape of the demarcation line. Even in these cases projection populations are much closer to IBP than are Mulliken populations, for example. IPP and IPP2 still give a reasonable qualitative description of the charge transfer. The application of integrated projection populations is justified by the efficiency of the integration. The sequence projection/demarcation/two-dimensional integration can be computed much faster[65] than the sequence demarcation/three-dimensional integration.

It is my pleasure to thank Professors Andrew Streitwieser, Jr. and Kenneth B. Wiberg. Their generosity has enabled me to conduct this independent research. I also gratefully acknowledge support by the Verband der Chemischen Industrie, Federal Republic of Germany.

References

1. R. S. Mulliken, *J. Chem. Phys.*, **23**, 1833, 1848, 2338, 2343 (1955).
2. R. E. Davidson, *J. Chem. Phys.*, **46**, 3320 (1967).
3. K. R. Roby, *Mol. Phys.*, **27**, 81 (1974).
4. (a) Review: R. Ahlrichs and C. Ehrhardt, *Chem. Unserer Zeit*, **19**, 120 (1985). (b) C. Ehrhardt and R. Ahlrichs, *Theor. Chim. Acta*, **68**, 231 (1985). (c) R. Heinzmann and R. Ahlrichs, R., *Theoret. Chim. Acta*, **42**, 33 (1976).
5. (a) A. E. Reed, R. B. Weinstock, and F. Weinhold, *J. Chem. Phys.*, **83**, 735 (1985). (b) A. E. Reed, F. Weinhold, L. A. Curtiss, and D. J. Pochatko, *J. Chem. Phys.*, **84**, 5687 (1986). (c) A. E. Reed and F. Weinhold, *J. Chem. Phys.*, **78**, 4066 (1983).
6. See for example: (a) C. W. Kern and M. Karplus, *J. Chem. Phys.*, **40**, 1374 (1964). (b) P. Politzer and L. C. Cusachs, *Chem. Phys. Lett.*, **2**, 1 (1968). (c) C. A. Coulson and G. Doggett, *Int. J. Quantum Chem.*, **2**, 823 (1968). (d) G. Doggett, *J. Chem. Soc. A*, 229 (1969).
7. Compare Refs. 5, 33, and 38a,c.
8. For an impressive example see: R. S. Mulliken, *J. Chem. Phys.*, **36**, 3428 (1962).
9. T. Ros and G. C. A. Schuit, *Theoret. Chim. Acta*, **4**, 1 (1966).
10. E. W. Stout, Jr. and P. Politzer, *Theoret. Chim. Acta*, **12**, 379 (1968).
11. (a) P. Politzer and R. R. Harris, *J. Am. Chem. Soc.*, **92**, 6451 (1970). (b) P. Politzer and R. S. Mulliken, *J. Chem. Phys.*, **55**, 5135 (1971). (c) P. Politzer and P. H. Reggio, *J. Am. Chem. Soc.*, **94**, 8308 (1972).
12. R. E. Brown and H. Shull, *Int. J. Quantum Chem.*, 663 (1968).
13. P. Russegger and P. Schuster, *Chem. Phys. Lett.*, **19**, 254 (1973).
14. H. Lischka, *J. Am. Chem. Soc.*, **99**, 353 (1977).
15. See also: W. H. E. Schwarz, P. Valtazanos, and K. Ruedenberg, *Theoret. Chim. Acta*, **68**, 471 (1985) and references therein.
16. K. B. Wiberg, *J. Am. Chem. Soc.*, **102**, 1229 (1980).
17. (a) R. F. W. Bader, W. H. Henneker, and P. E. Cade, *J. Chem. Phys.*, **46**, 3341 (1967). (b) R. F. W. Bader, I. Keaveny, and P. E. Cade, *J. Chem. Phys.*, **47**, 3381 (1967). (c) R. F. W. Bader, I. Keaveny, and G. Runtz, *Can. J. Chem.*, **47**, 2308 (1969). (d) P. E. Cade, R. F. W. Bader, W. H. Henneker, and I. Keaveny, *J. Chem. Phys.*, **50**, 5313 (1969).
18. R. F. W. Bader, P. M. Beddall, and P. E. Cade, *J. Am. Chem. Soc.*, **93**, 3095 (1971).
19. R. F. W. Bader and P. M. Beddall, *J. Chem. Phys.*, **56**, 3320 (1972).
20. (a) R. F. W. Bader and P. M. Beddall, *J. Am. Chem. Soc.*, **95**, 305 (1973). (b) R. F. W. Bader, P. M. Beddall, and J. Peslak, Jr., *J. Chem. Phys.*, **58**, 557 (1973). (c) R. F. W. Bader and R. R. Messer, *Can. J. Chem.*, **52**, 2268 (1974). (d) R. F. W. Bader, *Acc. Chem. Res.*, **8**, 34 (1975).
21. G. R. Runtz, R. F. W. Bader, and R. R. Messer, *Can. J. Chem.*, **55**, 3040 (1977).
22. (a) S. Srebrenik and R. F. W. Bader, *J. Chem. Phys.*, **63**, 3945 (1975). (b) R. F. W. Bader and T. T. Nguyen-Dang, *Adv. Quantum Chem.*, **14**, 63 (1981). (c) S. Srebrenik, R. F. W. Bader, and T. T. Nguyen-Dang, *J. Chem. Phys.*, **68**, 3667, 3680 (1978).
23. (a) R. F. W. Bader, S. G. Anderson, and A. J. Duke, *J. Am. Chem. Soc.*, **101**, 1389 (1979). (b) R. F. W. Bader, T. T. Nguyen-Dang, and Y. Tal, *J. Chem. Phys.*, **70**, 4316 (1979).
24. (a) R. F. W. Bader, *J. Chem. Phys.*, **76**, 2871 (1980). (b) Review: R. F. W. Bader, T. T. Nguyen-Dang, and Y. Tal, *Rep. Prog. Phys.*, **44**, 893 (1981).
25. F. W. Biegler-König, R. F. W. Bader, and T.-H. Tang, *J. Comput. Chem.*, **3**, 317 (1982).
26. R. F. W. Bader, T.-H. Tang, Y. Tal, and F. W. Biegler-König, *J. Am. Chem. Soc.*, **104**, 940, 946 (1982).
27. R. F. W. Bader, T. S. Lee, D. Cremer, and E. Kraka, *J. Am. Chem. Soc.*, **105**, 5061 (1983).
28. (a) D. Cremer, E. Kraka, T. S. Slee, R. F. W. Bader, C. D. H. Lau, T. T. Nguyen-Dang, and P. J. MacDougall, *J. Am. Chem. Soc.*, **105**, 5069 (1983). (b) R. F. W. Bader, P. J. MacDougall, and C. D. H. Lau, *J. Am. Chem. Soc.*, **106**, 1594 (1984). (c) R. F. W. Bader and H. Essen, *J. Chem. Phys.*, **80**, 1943 (1984). (d) R. F. W. Bader and P. J. MacDougall, *J. Am. Chem. Soc.*, **107**, 6788 (1985).
29. Reviews: (a) R. F. W. Bader, *Acc. Chem. Res.*, **18**, 9 (1985). (b) R. F. W. Bader, *Pure Appl. Chem.*, **60**, 145 (1988).
30. T.-H. Tang, R. F. W. Bader, and P. J. MacDougall, *Inorg. Chem.*, **24**, 2047 (1985).
31. (a) R. F. W. Bader, *Can. J. Chem.*, **64**, 1036 (1986). (b) P. J. MacDougall, R. F. W. Bader, *Can. J. Chem.*, **64**, 1496 (1986). (c) R. F. W. Bader, A. Larouche, C. Gatti, M. T. Carrroll, P. J. MacDougall, and K. B. Wiberg, *J. Chem. Phys.*, **87**, 1142 (1987). (d) R. F. W. Bader and K. B. Wiberg, *Density Matrices and Density Functions* (Proc. A), R. Erdahl and V. H. Smith, Jr. (Eds.), Reidel: Dordrecht, The Netherlands, 1987, p. 677. (e) R. F. W. Bader, M. T. Carroll, and J. R. Cheeseman, *J. Am. Chem. Soc.*, **109**, 7968 (1987). (f) W. L. Cao, C. Gatti, P. J. MacDougall, and R. F. W. Bader, *Chem. Phys. Lett.*, **141**, 380 (1987).
32. (a) K. B. Wiberg and J. J. Wendoloski, *Proc. Natl. Acad. Sci. (USA)*, **78**, 6561 (1981). (b) K. B.

Wiberg, R. F. W. Bader, and C. D. H. Lau, *J. Am. Chem. Soc.*, **109**, 985, 1001 (1987). (c) K. B. Wiberg and K. E. Laidig, *J. Am. Chem. Soc.*, **109**, 5935 (1987).
33. A. Streitwieser, Jr., J. E. Williams, S. Alexandratos, and J. M. McKelvey, *J. Am. Chem. Soc.*, **98**, 4778 (1976).
34. J. B. Collins, A. Streitwieser, Jr., and J. M. McKelvey, *Comput. Chem.*, **3**, 79 (1979).
35. A. Streitwieser, Jr., J. B. Collins, J. M. McKelvey, D. L. Grier, J. Sender, and A. G. Toczko, *Proc. Natl. Acad. Sci. (USA)*, **76**, 2499 (1979).
36. Review: A. Streitwieser, Jr., D. L. Grier, B. A. B. Kohler, E. R. Vorpagel, and G. W. Schriever, *Electron Distributions and the Chemical Bond*, P. Coppens and M. Hall (Eds.), Plenum Press, New York, 1982.
37. R. S. McDowell, D. L. Grier, and A. Streitwieser, Jr., *Comput. Chem.*, **9**, 165 (1985).
38. (a) D. L. Grier and A. Streitwieser, Jr., *J. Am. Chem. Soc.*, **104**, 3556 (1982). (b) A. Streitwieser, Jr., C. M. Berke, G. W. Schriver, D. Grier, and J. B. Collins, *Tetrahedron (Suppl.)*, **9**, 345 (1981). (c) J. B. Collins and A. Streitwieser, Jr., *J. Comput. Chem.*, **1**, 81 (1980). (d) R. S. McDowell and A. Streitwieser, Jr., *J. Am. Chem. Soc.*, **106**, 4047 (1984). (e) S. M. Bachrach and A. Streitwieser, Jr., *J. Am. Chem. Soc.*, **106**, 5818 and 2283 (1984). (f) S. M. Bachrach and A. Streitwieser, Jr., *J. Am. Chem. Soc.*, **107**, 1186 (1985). (g) S. M. Bachrach and A. Streitwieser, Jr., *J. Am. Chem. Soc.*, **108**, 3946 (1986). (h) D. A. Bors and A. Streitwieser, Jr., *J. Am. Chem. Soc.*, **108**, 1397 (1986). (i) A. Streitwieser, Jr. and R. S. McDowell, *J. Mol. Struct. THEOCHEM*, **31**, 89 (1986). (j) A. Streitwieser, Jr., R. S. McDowell, and R. Glaser, *J. Comput. Chem.*, **8**, 788 (1987). (k) E. Kaufmann, P. v. R. Schleyer, S. Gronert, A. Streitwieser, Jr., and M. Halpern, *J. Am. Chem. Soc.*, **109**, 2533 (1987). (l) A. Streitwieser, Jr., A. Rajca, R. S. McDowell, and R. Glaser, *J. Am. Chem. Soc.*, **109**, 4184 (1987). (m) S. Gronert, R. Glaser, and A. Streitwieser, Jr., *J. Am. Chem. Soc.*, submitted for publication.
39. (a) R. Glaser and A. Streitwieser, Jr., *Pure & Appl. Chem.*, **60**, 195 (1988). (b) R. Glaser and A. Streitwieser, Jr., *J. Am. Chem. Soc.*, submitted.
40. (a) D. Cremer and E. Kraka, *Croat. Chem. Acta*, **57**, 1259 (1984). (b) D. Cremer and E. Kraka, *J. Am. Chem. Soc.*, **107**, 3800 and 3811 (1985). (c) W. Koch, G. Frenking, J. Gauss, D. Cremer, A. Sawaryn, and P. v. R. Schleyer, *J. Am. Chem. Soc.*, **108**, 5732 (1986).
41. Cremer and Kraka showed that bond paths can occur between two bond critical points; cf. Ref. 40b. See also Refs. 31f and 43.
42. (a) K. Collard and G. G. Hall, *Int. J. Quantum Chem.*, **12**, 623 (1977). (b) V. H. Smith, I. Absar, *Israel J. Chem.*, **16**, 187 (1977).
43. (a) J. S. Ritchie and S. M. Bachrach, *J. Comput. Chem.*, **8**, 499 (1987). (b) J. S. Ritchie and S. M. Bachrach, *J. Am. Chem. Soc.*, **109**, 5909 (1987).
44. M. Simonetta, M. Barzaghi, and C. Gatti, *J. Mol. Str. THEOCHEM*, **138**, 39 (1986).
45. (a) R. J. Boyd and S. C. Choi, *Chem. Phys. Lett.*, **120**, 80 (1985). (b) R. J. Boyd and S. C. Choi, *Chem. Phys. Lett.*, **129**, 62 (1986).
46. Integrated Projection Populations (IPP) were introduced as Integrated Spatial Electron Populations, ISEP (Ref. 35), and they were renamed recently.
47. The analogy is not general. This description of $P(x,z)$ is advantageous for planar molecules if the molecular plane coincides with the plane of projection (e.g., all systems considered in this paper) because it facilitates the comparison of topological features of $P(x,z)$ and $\rho(r)$ and of the partitioning methods.
48. RHF/6-31G* wavefunction, cf. section Computational Aspects.
49. Positions of critical points as determined from grid data calculated with PROJ. The locations of bond critical points depend slightly on whether they are determined by interpolation of grid data or by a NR-walk; see section Computational Aspects.
50. The derivations of the relations between the integrated populations does not require any consideration of AOs or MOs. Here, components of the electron density are separated for an interpretation in more familiar terms. The argument does not rely on this separation; the same argument could be made considering the dependence of the electron density on the distance from the internuclear axis. Electron density that is farther away from the axis is more polarizable.
51. J. S. Binkley, M. J. Frisch, D. J. DeFrees, K. Raghavachari, R. A. Whiteside, H. B. Schlegel, E. M. Fluder, and J. A. Pople, Carnegie-Mellon University, Pittsburg, Pennsylvania, 1985.
52. W. J. Hehre, R. Ditchfield, and J. A. Pople, *J. Chem. Phys.*, **56**, 2257 (1972). P. C. Hariharan, and J. A. Pople, *Theoret. Chim. Acta*, **28**, 213 (1973). J. S. Binkley, M. S. Gordon, D. J. DeFrees, and J. A. Pople, *J. Chem. Phys.*, **77**, 3654 (1982).
53. J. Chandrasekhar, J. G. Andrade, and P. v. R. Schleyer, *J. Am. Chem. Soc.*, **103**, 5609 (1981).
54. *The Carnegie-Mellon Quantum Chemistry Archive*, 3rd Ed., R. A. Whiteside, M. J. Frisch, and J. A. Pople, (Eds.) Carnegie-Mellon University, Pittsburgh, Pennsylvania, 1983.
55. R. Glaser and A. Streitwieser, Jr., *J. Am. Chem. Soc.*, **109**, 1258 (1987).
56. F. W. Biegler-König, McMaster University, Hamilton, Ontario, 1980.
57. F. W. Biegler-König and J. A. Duke, McMaster University, Hamilton, Ontario, 1981. Modifications by C. D. H. Lau, McMaster University, Hamilton, Ontario, 1983. Adapted for a CSPI array processor by T. J. LePage, Yale University, New Haven, Connecticut, 1987. See also Ref. 25.
58. For a study of LiF, compare: A. Hinchliffe and J. C. Dobson, *Chem. Soc. Rev.*, **5**, 79 (1976).
59. Both, IPP and IPP2 equal IBP in the limit of a homonuclear diatomic. Their deviations from IBP in dependance of the bond polarity are different. It is in this sense that IPP2 represents the better approximation for molecules of low but significant bond polarity.
60. Supplemental Material (21 pages) available from the author: Structures and energies of 1–6. Contour plots of the electron density and of the projection functions of 2–6 and of the diatomic molecules. Bond properties (r_A, r_B, F3, λ_i, $\nabla^2(\rho)$, ε) of the diatomic molecules (Table VI) and of 1–6 (Table VIII), and atomic properties (IBP$_\pi$, L, T′, T″) of the diatomic molecules (Table VII) and of 1–6 (Table IX).
61. For a study of 4, see: P. v. R. Schleyer, *J. Am. Chem. Soc.*, **107**, 4793 (1985).
62. For electron density analyses of 1,4 and related compounds, compare: K. B. Wiberg, C. M. Brene-

man, T. J. LePage, M. Frisch, and R. Glaser, manuscript in preparation.
63. For discussions SiH bond polarities, see Refs. 31c and 38m.
64. Projection populations and IBP of silane and of silaethene agree well: A. Streitwieser, Jr., private communication.
65. Benchmark: p,p-Diaminovinyldiazonium cation (I, planar) at RHF/6-31G* (100 bfs, 188 prim.). Integrations over the 11 basins required 26.79 h (average 2.43 h/integration) on the array processor. Calculation of $P(x,z)$ of I using an enhanced version of PROJ (ISEP by B. Tansy, A. Streitwieser, Jr.) for a squared grid (16 a.u., spacing 0.2 au.) required 1.47 h on a MicroVax II. (Time required for integrations of regions of $P(x,z)$ is marginal.) Proaims runs about 12 times faster on the array processor than on the MicroVax II. Thus, in this case the calculation of $P(x,z)$ is 20 times faster than one run of Proaims!